Droplets passing through a soap film

Jun Zou, Wei Wang, Chen Ji, and Min Pan

Citation: Physics of Fluids **29**, 062110 (2017); doi: 10.1063/1.4986798
View online: http://dx.doi.org/10.1063/1.4986798
View Table of Contents: http://aip.scitation.org/toc/phf/29/6
Published by the American Institute of Physics

Droplets passing through a soap film

Jun Zou,[1,a)] Wei Wang,[1] Chen Ji,[1,b)] and Min Pan[2]
[1]*State Key Laboratory of Fluid Power and Mechatronic Systems, Zhejiang University, Hangzhou 310027, China*
[2]*Center for Power Transmission and Motion Control, Department of Mechanical Engineering, University of Bath, Bath BA2 7AY, United Kingdom*

(Received 12 January 2017; accepted 6 June 2017; published online 22 June 2017)

Here, we report an experimental study of droplets colliding with a soap film. The behavior of the droplet is found to be dependent on the impact velocity. The threshold for a droplet to pass through the soap film is influenced by the droplet diameter. The contact time decreases with increasing impact velocity. Emphasis is placed on whether the outer shell remains intact. When the dimensionless contact time approaches 1, collapse of the shell begins. However, the shell does not collapse with further increasing impact velocity. *Published by AIP Publishing.* [http://dx.doi.org/10.1063/1.4986798]

I. INTRODUCTION

Collision of droplets with various substances has been widely investigated. These substances include solid plates (hydrophilic or hydrophobic),[1–3] liquid baths (miscible or immiscible),[4–8] and powder surfaces.[9,10] Diverse phenomena have been reported, for instance, bouncing, floating, splashing, jetting, and bubble entrainment.[11–13]

When a high-speed water drop collides with a superhydrophobic solid plate, it can completely bounce back.[14] During the collision, the maximal deformation of the drop increases with increasing impact velocity, while the contact time remains constant in most cases.[2,15] Analogous results have been reported when a water drop collides with a liquid bath.[5,6] Interestingly, a powder surface also acts as a superhydrophobic plate, enabling a colliding droplet to completely bounce back.[9]

One of the targets of interest is a suspended soap film. When a droplet collides with a static soap film, it undergoes bouncing or coalescence (total or partial coalescence), or totally passes through the soap film. The phenomenon depends on the Weber number $We = \rho v^2 d/\sigma$, where v is the impacting velocity and ρ, d, and σ represent the density, the diameter, and the surface tension of the drop, respectively. At a Weber number high enough, it was widely reported that the droplet could totally pass through the soap film without transferring any liquid into the soap film. In the case of soap droplets, Fell *et al.*[17] observed this "total passing" around $We = 12$, which is lower than the result of $We \approx 16$ reported by Gilet and Bush.[16] This discrepancy was attributed to the less viscous soap solution used by Fell *et al.* to produce the soap films.[17] In the case of pure water droplet, the corresponding Weber number was found to be about 6.[17] Thoroddsen *et al.*[18] employed a hemisphere-shaped soap film as the impacting target of the water drop, and they observed total passing at a higher Weber number ($We \approx 16$). However, previous works also reported that the phenomenon was unpredictable in this region of the Weber number. Droplets with the same Weber number led to various phenomena, including bounce, coalescence, partial coalescence, and total passing. The probability of different results was presented as a function of the Weber number.[16,17] A further increase of the Weber number prevented this uncertainty, and every impinging droplet totally passed through the soap film. This critical value of the Weber number was reported as 25.1[16] or 20.[17]

On the phenomenon of total passing, it is worth noting that the soap film will not break after the drop passes through it, but will go through a "self-healing" process.[29] This process was employed by Bai *et al.*[19] to develop a feasible method to produce antibubbles. An antibubble is a fluid particle consisting of a liquid globule and a surrounding air film,[20] which has attracted great attention in the last decade.[21–26] In the method of Bai *et al.*, a droplet released from a needle firstly collided with a soap film and passed through it, then deposited onto a liquid pool. After passing through the soap film, it was found that the droplet was packed by a liquid outer shell with an air layer separating them; thus, the later collision with the pool could produce an antibubble.[19] As Thoroddsen *et al.*[18] reported, the outer shell might collapse during the falling process of the drop. However, the experiments in previous studies were limited in $We < 30$, and the behavior of the drop after passing through the film was not investigated systemically.

The system of a liquid drop impacting a suspended film was believed to have many potential applications in the future.[27–29] In this study, we aim to investigate the collision of a soap droplet with a soap film in a high-We region. The focus was the phenomena after the droplet totally passing through the film. With the aid of a high-speed camera, the details of the collisions were captured. The experimental results were presented and elucidated, and then the mechanism leading to maintenance or collapse of the liquid shell was discussed.

II. EXPERIMENTAL SETUP

The left part of Fig. 1 shows the experimental setup. Droplets were generated by a syringe with flat tipped stainless needles of various diameters. They then fell onto the center of a round soap film with an internal diameter of $D = 2$ cm, which

[a)]junzou@zju.edu.cn
[b)]jich@zju.edu.cn

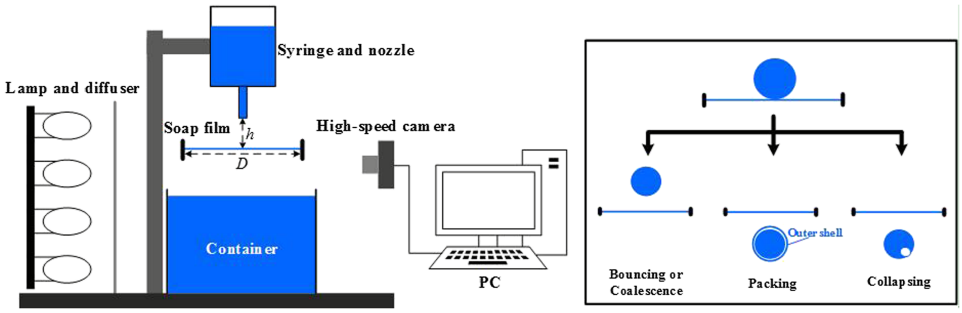

FIG. 1. The left part presents the experimental setup used in the experiments. The high-speed camera worked at 20 000 fps. The right part indicates three kinds of experimental results: bouncing or coalescence, packing, and collapsing.

was fixed by a ring of copper wire. The soap film was produced by extracting the ring out of a container (100 mm × 100 mm × 100 mm) filled with a soap solution. Then the film thins gradually due to the evaporation. To make sure that the soap film thickness is equivalent for each collision, we uniformly captured the impact 10 s after the films were generated. Moreover, the film was renewed after each collision. To measure the thickness of the film δ, we punctured the film with a dry stainless needle, forming a hole on the film. Note that, the film was also punctured 10 s after its formation. Then the growth rate v_r of the hole was recorded. During the collapse, the balance between surface tension and inertia leads to a velocity $v_r = (2\sigma/\rho\delta)^{1/2}$, where σ and ρ are the surface tension and density, respectively.[30] Eight films were measured and δ ranged from 8 μm to 12 μm.

Both the droplet and the soap film were prepared with a mixture of tap water and commercial soap whose critical ingredient is sodium dodecyl benzene sulfonate (SDBS). The concentration of the soap was 1% by volume. We measured the surface tension of the soap solution with a glass capillary tube of inner diameter $r = 0.5$ mm. The surface tension σ was 30 ± 2 mN/m. The density ρ was about 1000 kg/m^3.

A high-speed camera (Phantom, UHS-12, V2512) with a Nikkor 60-mm lens was used to capture the details of the impact (frame rate 20 000 fps). The background light was produced by a high-intense LED lamp (100 W) and diffused by a sheet of drafting paper. The impact velocity was calculated as the free falling motion $v = [2g(h - d)]^{1/2}$, where h is the vertical distance from the target surface to the needle tip and d is the droplet diameter. We compared this value with the velocity calculated using the high-speed camera videos. The deviation was about 5%. The experiments were carried out at laboratory temperature (25 ± 2 °C). The variation of the fluid parameters caused by temperature perturbation was negligible.

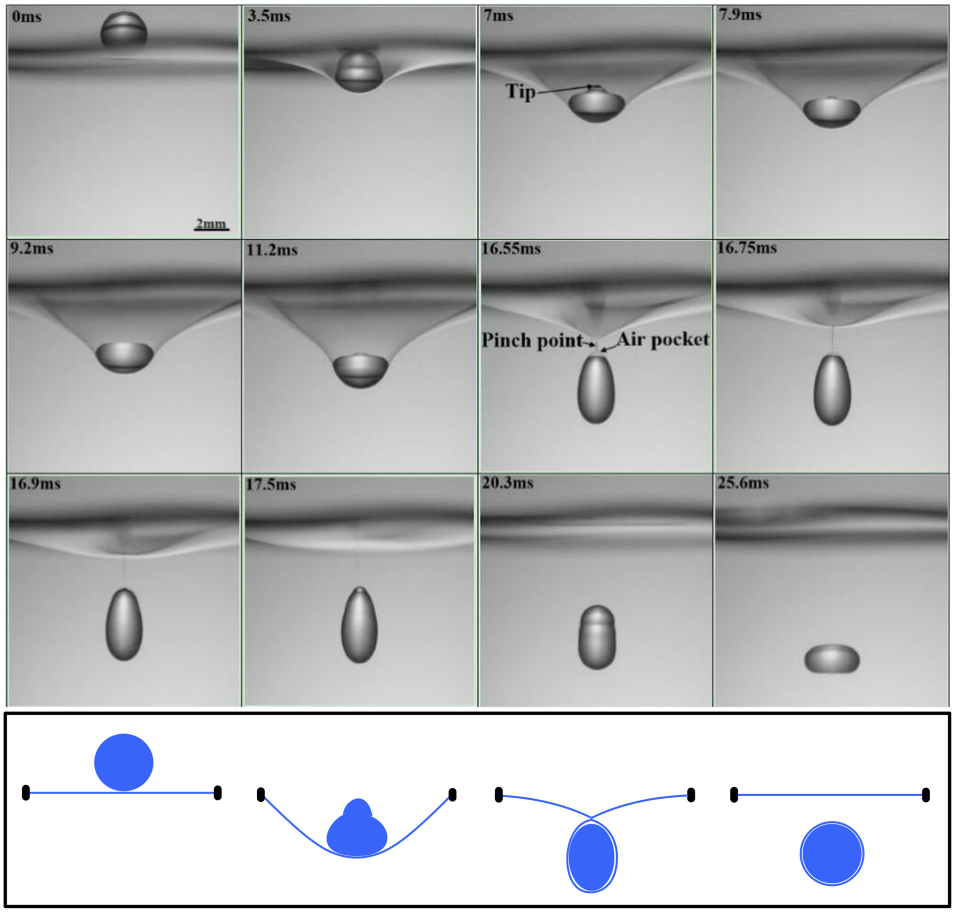

FIG. 2. Droplet ($d = 2.65$ mm, $v = 0.67$ m/s and $We = 39.49$) colliding with and passing through a soap film with an outer shell. This shell remains intact while the droplet vibrates in the air. The schematic is depicted according to the experimental results. (Multimedia view) [URL: http://dx.doi.org/10.1063/1.4986798.1]

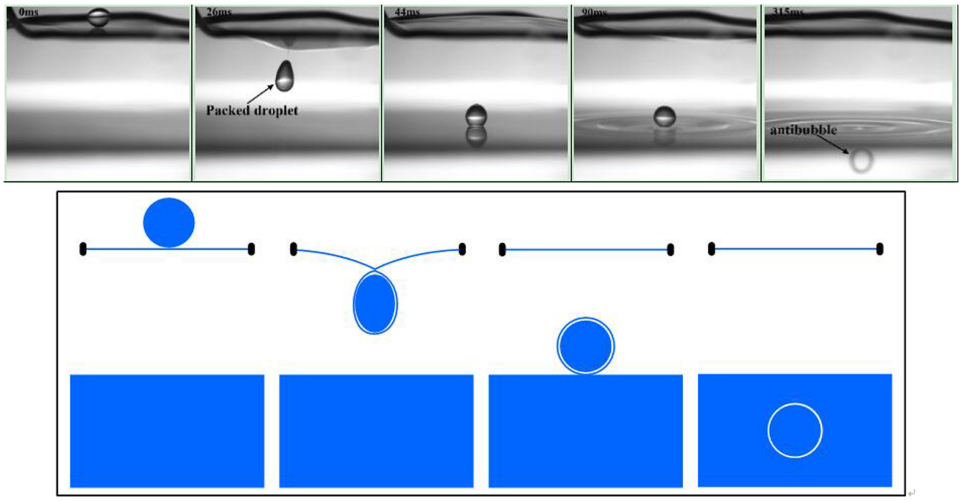

FIG. 3. Formation of an antibubble after the droplet passing through the soap film. (Multimedia view) [URL: http://dx.doi.org/10.1063/1.4986798.2]

Every experiment was repeated for 5 times to validate the phenomenon. The schematic in the right part of Fig. 1 presents three kinds of collision results. In the present work, all the cases that the droplet does not totally pass through the film are counted as one category named as "bouncing or coalescence." In the cases of total passing, the droplet passes through the soap film without partial coalescence. Depending on the maintenance or collapse of the outer shell (as indicated in Fig. 1), this condition was classified into two categories named "packing" and "collapsing," respectively.

III. RESULTS

When the impact velocity is sufficiently low, the droplet may coalesce with the soap film or completely bounce back. However, high-speed droplets can totally pass through the soap film without breaking it.[16,17]

Figure 2 (Multimedia view) shows the image sequence of a droplet ($d = 2.65$ mm, $v = 0.67$ m/s and $We = 39.49$) totally passing through a soap film. $t = 0$ indicates the time at which the droplet begins to deform the soap film. When the droplet collides with the soap film, the film deforms into a pocket around the drop. This pocket then pinches off at the top

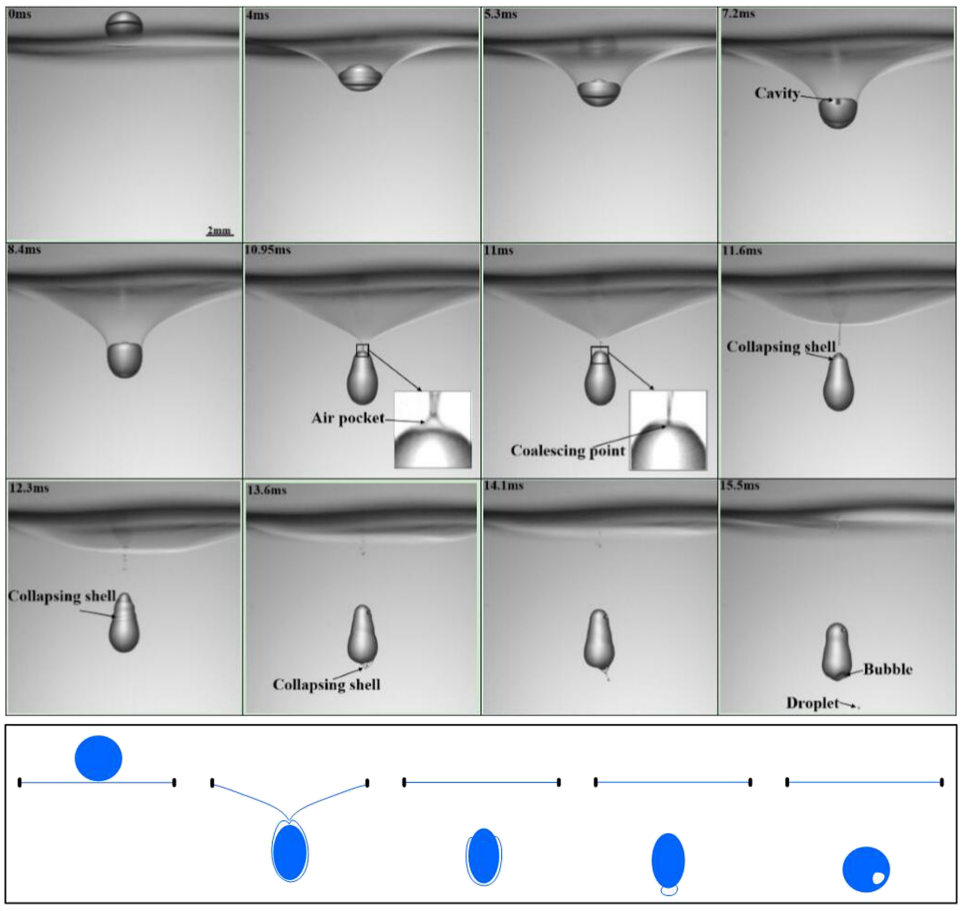

FIG. 4. Droplet passing through a soap film, $d = 2.65$ mm, $v = 0.99$ m/s and $We = 87.19$. The outer film begins to collapse after passing through the soap film. The coalescence point between the droplet and the outer shell is shown. The schematic is depicted according to the experimental results. (Multimedia view) [URL: http://dx.doi.org/10.1063/1.4986798.3]

($t = 16.55$ ms), forming a liquid shell packing the droplet. A thin layer of air separates the shell from the droplet, and a pocket of air is trapped on the top ($t = 16.55$ ms). At the same time, capillary waves caused by the impact travel along the droplet surface and converge at the top of the droplet, resulting in a tip ($t = 7$ ms). Subsequently, the tip shrinks into the droplet. Then a thick jet emerges on the top of the droplet ($t = 11.2$ ms). This time is denoted as t_J which ranges from the moment when the soap film starts to deform to that when the droplet starts to elongate vertically. This process is similar to deformation of a drop colliding with a super-hydrophobic plate.[2] After separating from the soap film, a packed droplet is generated with a thin air layer separating the droplet and the outer shell. This shell remains intact while the droplet vibrates in air. The schematic below the image sequence depicts the collision process according to the experimental results.

Note that, an antibubble is generated when the packed droplet impacts onto the soap solution pool.[22] Figure 3 (Multimedia view) presents both the images and schematics indicating the formation of an antibubble. The packed droplet rests on the pool after the impact and then the outer shell coalesces with the pool. The soap droplet is pushed into the pool, giving rise to the formation of an antibubble. This phenomenon verifies the existence of the continuous air layer.

Increasing the impact velocity results in collapse of the outer shell. As shown in Fig. 4 (Multimedia view), the droplet ($d = 2.65$ mm, $v = 0.99$ m/s and $We = 87.19$) is surrounded by a closed shell when passing through the soap film ($t = 10.95$ ms). However, the air pocket on the top is almost invisible [comparing with Fig. 2 (Multimedia view)]. After pinch-off, the shell contracts downwards and touches the top surface of the droplet, leading to their coalescence ($t = 11$ ms). The outer shell collapses and propagates down the droplet. At the bottom, the shell assembles and ejects a tiny droplet ($t = 14.1$ ms). Finally, the film evolves into a bubble that is entrapped in the droplet ($t = 15.5$ ms). Analogous phenomena occurred when a water drop passed through a soap film.[18] Coalescence between the water drop and the surrounding soap shell led to the collapse of this shell. A jet was ejected out at the bottom of the water drop, which was driven by the surface tension difference between the water drop and the soap shell. In our experiments, both the droplet and the soap film were generated with the same soap solution. Therefore, no jet was observed to emerge at the bottom of the droplet. The ejection presented ($t = 14.1$ ms) emerged on the bubble instead of the droplet.

The schematic below the image sequence depicts the collision process according to the experimental results. Coalescence between the outer shell and the droplet is highlighted.

Figure 5 (Multimedia view) shows another mechanism for the collapse of the outer shell. In this case, the corresponding parameters are: $d = 2.65$ mm, $v = 1.25$ m/s and $We = 138.42$. In contrast to Fig. 4 (Multimedia view), the air

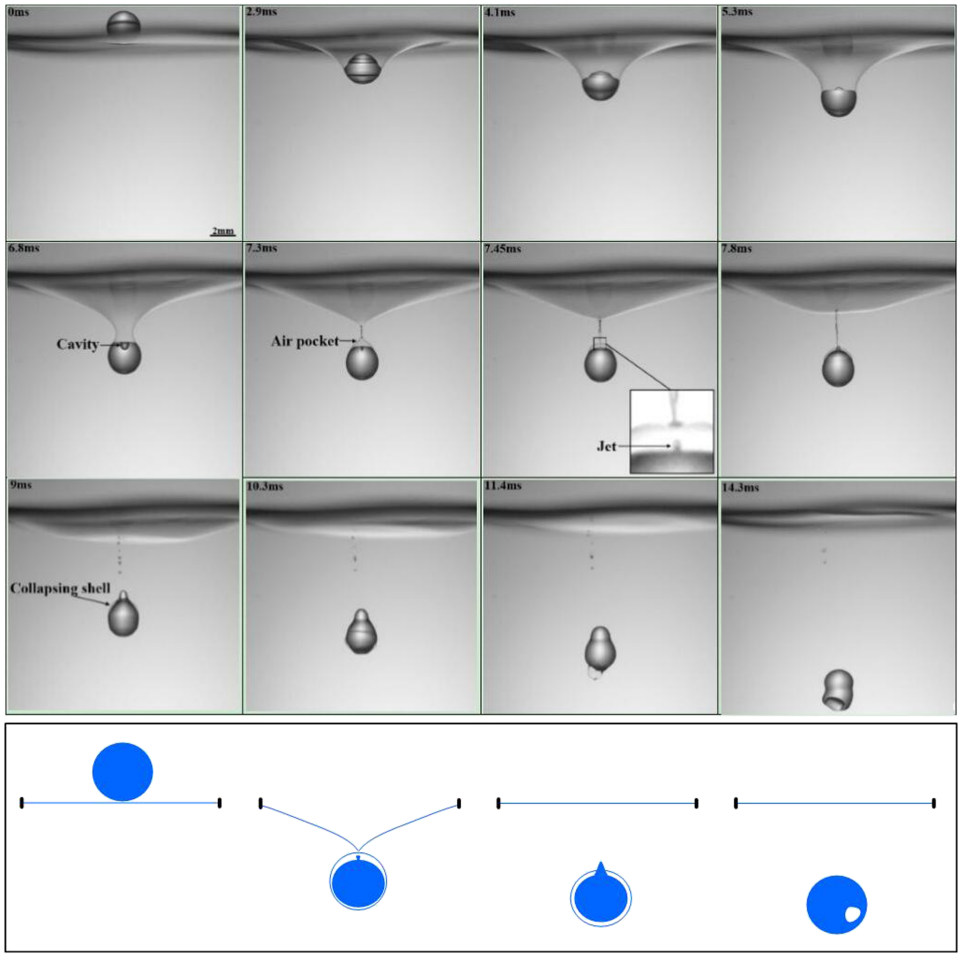

FIG. 5. Droplet passing through a soap film, $d = 2.65$ mm, $v = 1.25$ m/s and $We = 138.42$. The outer shell collapses duo to the emergence of a jet on the top of the droplet. The schematic is depicted according to the experimental results. (Multimedia view) [URL: http://dx.doi.org/10.1063/1.4986798.4]

pocket here is sufficiently large to prevent the outer shell from collapsing owing to coalescence ($t = 7.3$ ms). However, a jet is formed ($t = 7.45$ ms) on the top of the droplet by the convergence of the capillary waves, and it punctures the outer shell ($t = 7.8$ ms). Subsequently, the broken shell propagates down the droplet and evolves into a bubble entrapped in the droplet ($t = 14.3$ ms).

The schematic below the image sequence depicts the collision process according to the experimental results. Emergence of the jet on the top of the droplet is presented.

Before the emergence of the jet, a cavity forms at the top of the droplet. This cavity results from the sinking tip [Figs. 4 ($t = 7.2$ ms) and 5 ($t = 6.8$ ms) (Multimedia view)]. Figure 6 (Multimedia view) shows that the cavity pinches into a small bubble inside the droplet ($t = 7.2$ ms). In this case, the corresponding parameters are: $d = 2.65$ mm, $v = 1.34$ m/s and $We = 159.62$. At the same time, a high-speed thin jet is ejected out ($t = 7.4$ ms). Formation of the thin jet resembles the process of primary bubble entrainment when a droplet collides with a liquid bath.[4] Subsequently, the jet punctures the outer shell. The collapsing shell shrinks into a bubble entrapped in the droplet ($t = 15$ ms).

The schematic below the image sequence depicts the collision process according to the experimental results. Formation of a bubble in the droplet is presented.

Further increasing the impact velocity results in formation of a packed droplet again, as shown in Figs. 7 and 8 (Multimedia view). The parameters of the droplets in Figs. 7 and 8 (Multimedia view) are ($d = 2.65$ mm, $v = 1.48$ m/s, $We = 193.19$) and ($d = 2.65$ mm, $v = 2.05$ m/s, $We = 369.85$), respectively. Comparing Figs. 2 and 4–7 (Multimedia view), the air pocket significantly increases with increasing impact velocity. This prevents the outer shell from being punctured by the ejected jet. When the impact velocity reaches a certain value, the droplet slightly deforms and no bubble is entrapped [Fig. 8 (Multimedia view)]. This also benefits the stability of the outer shell. After pinch-off, the shell also contracts downwards, though no direct contact with the droplet occurs.

Schematics are also presented according to the experimental results in Figs. 7 and 8 (Multimedia view). Both schematics highlight the enlargement of the air pockets. The schematic in Fig. 7 (Multimedia view) shows that the jet fails to touch the outer shell. The schematic in Fig. 8 (Multimedia view) shows the packed droplet without any bubble.

Figure 9 shows a regime map of the experimental results. The results are divided into four regimes: bouncing or coalescence, packing I, collapsing, and packing II. In the present work, we gradually increased the impact velocity and repeat the experiment for 5 times. Firstly, the droplet might experience bouncing, coalescence, or partial coalescence, as reported by Gilet and Bush.[16] In the present work, all the phenomena except total passing are included in one regime, named as

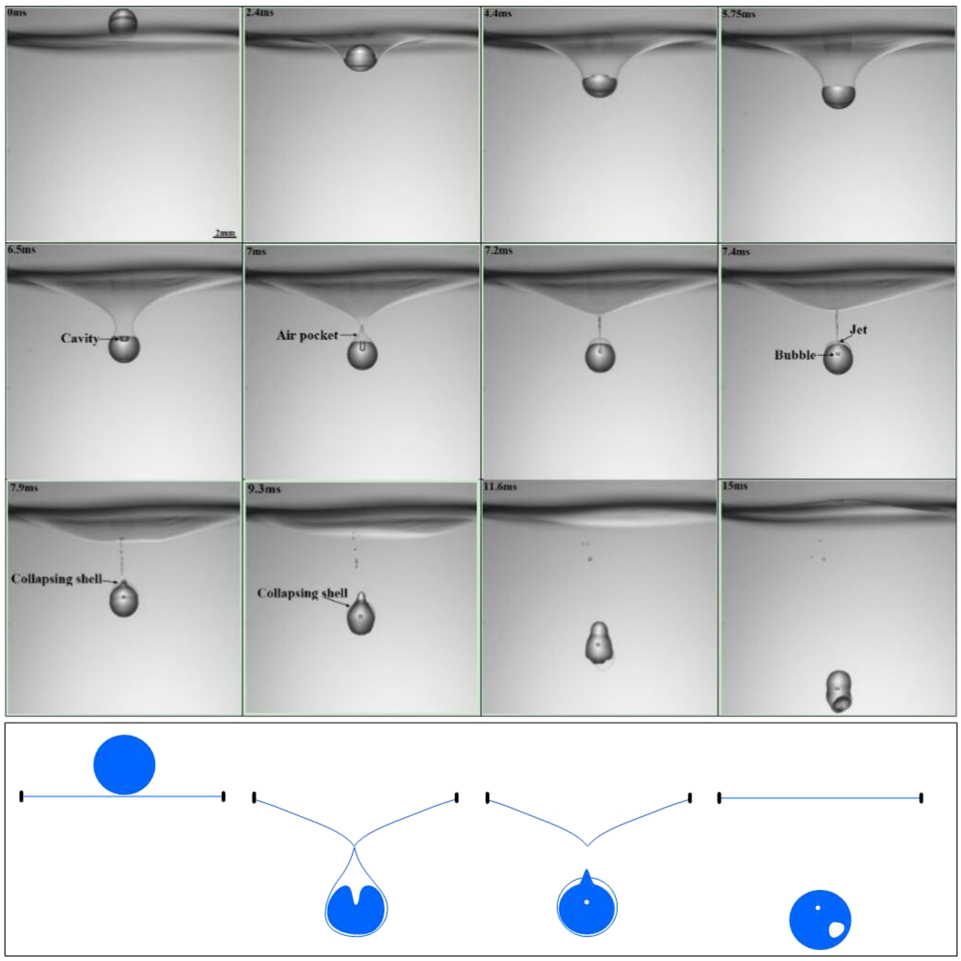

FIG. 6. Droplet passing through a soap film, $d = 2.65$ mm, $v = 1.34$ m/s and $We = 159.62$. A small bubble forms in the droplet. The schematic is depicted according to the experimental results. (Multimedia view) [URL: http://dx.doi.org/10.1063/1.4986798.5]

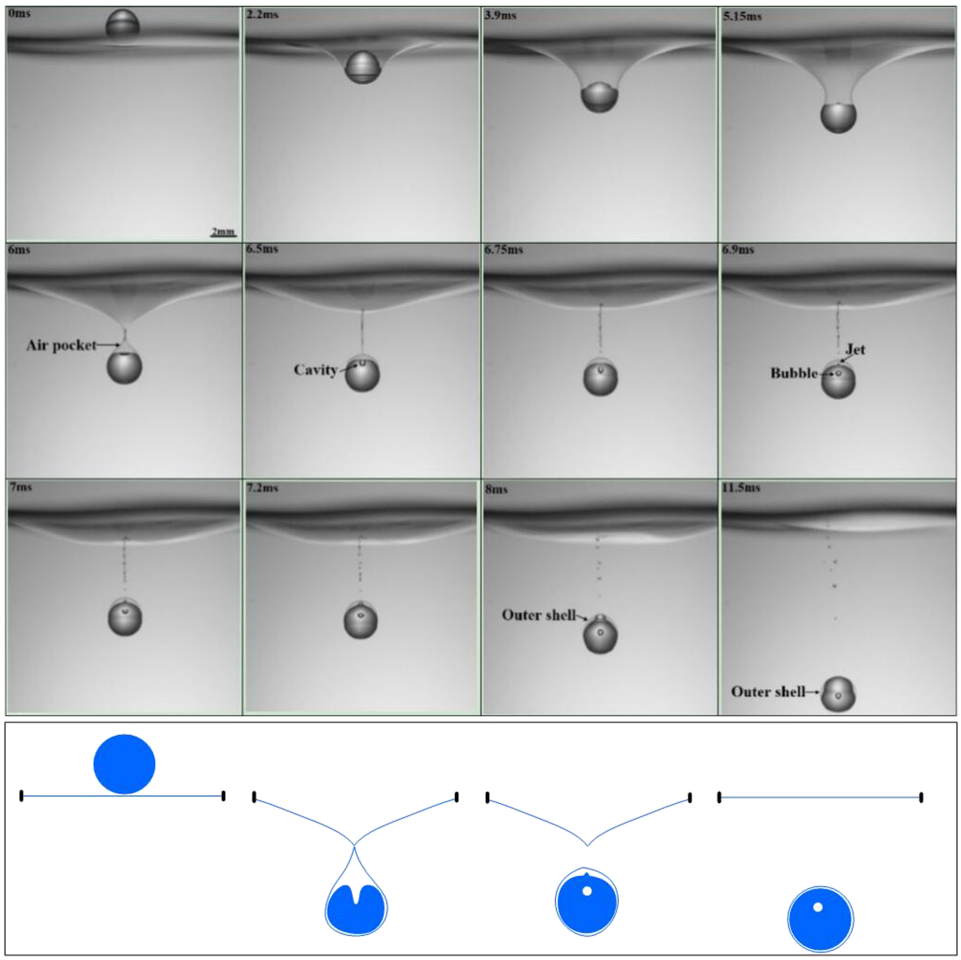

FIG. 7. Droplet passing through a soap film, $d = 2.65$ mm, $v = 1.48$ m/s, $We = 193.19$. A packed droplet forms. The schematic is depicted according to the experimental results. (Multimedia view) [URL: http://dx.doi.org/10.1063/1.4986798.6]

"bouncing or coalescence." Only if all the five drops successfully passed through the film without partial coalescence, we counted the result as "packing" or "collapsing." In this way, we obtained the critical Weber number We_c, which is the upper limit of the regime "bouncing or coalescence." Secondly, in the region of $(85 < We < 220)$, the droplet passes through the

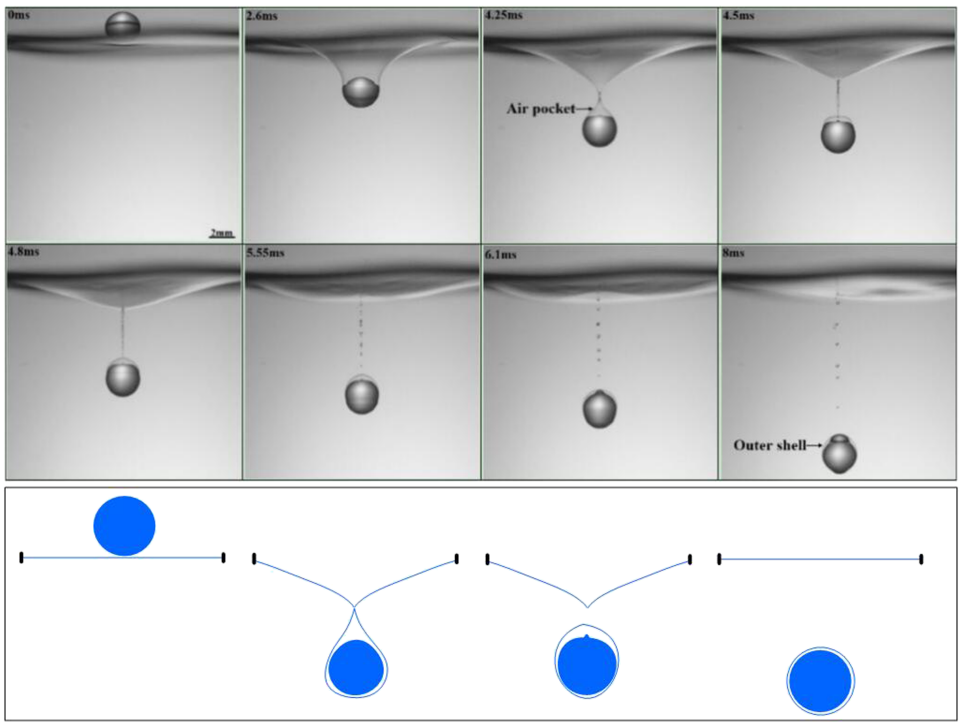

FIG. 8. Droplet passing through a soap film, $d = 2.65$ mm, $v = 2.05$ m/s, $We = 369.85$. A packed droplet forms without any bubbles. The schematic is depicted according to the experimental results. (Multimedia view) [URL: http://dx.doi.org/10.1063/1.4986798.7]

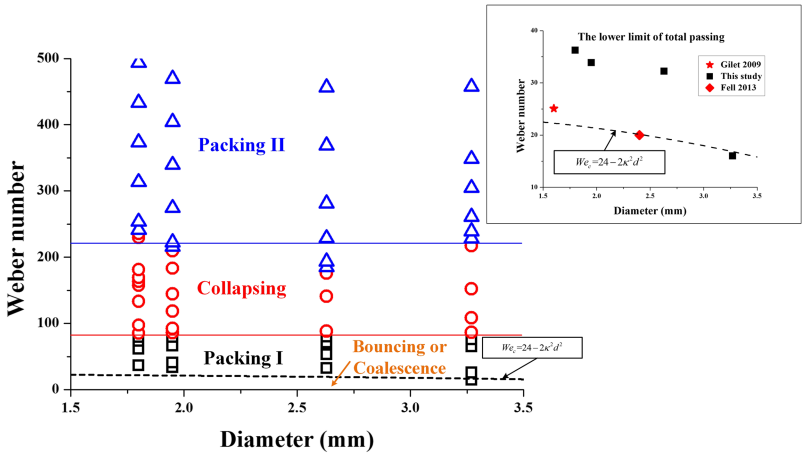

FIG. 9. Regime map of the experimental results. The black dashed line indicates the critical Weber number for passing: $We_c = 24 - 2\kappa^2 d^2$. This map is divided into four regimes: bouncing or coalescence, packing I, collapsing, and packing II. The inset presents the critical Weber number separating "bouncing or coalescence" and "packing I." The red star (d = 1.6 mm, We = 22) and diamond (d = 2.4 mm, We = 20) indicate the experimental results of Gilet and Fell, respectively. The black line in the inset is just for guide.

film with a surrounding liquid shell which subsequently collapses. This regime was defined as "collapsing." The third phenomenon is packing, which means that the drop totally passes through the film, and become a stable structure: liquid drop - air film - liquid shell, from inside out. Particularly, this structure appears in two separate regimes ($We_c < We < 85$) and ($220 < We < 500$), which are named as "packing I" and "packing II," respectively. Note that, "packing I" and "packing II" are defined based on the difference of the impact velocity. In both regimes, the droplets are packed after passing through the soap film. The critical Weber number separating the "bouncing or coalescence" and "packing I" regimes slightly decreases with increasing droplet diameter. The threshold between the "packing I" and "collapsing" regimes is around $We = 85$, and it is independent of the diameter. The droplet is packed again when the Weber number reaches a critical value of about 220.

The inset in Fig. 9 presents the critical Weber number We_c separating the "bouncing or coalescence" and "packing I," note that We_c corresponds to the value allowing every droplet to totally pass through the soap film. The red star ($d = 1.6$ mm, $We = 25.1$) and diamond ($d = 2.4$ mm, $We = 20$) indicate the experimental results of Gilet[16] and Fell,[17] respectively. Their results were observed using a soap film with $\delta \approx 1$ μm.[16,17] In comparison, δ ranges from 8 μm to 12 μm in the present work. It is reasonable that the thicker film leads to higher We_c, as the necessary energy to break the film increases with the thickness.

IV. DISCUSSION

The results in Fig. 9 show that the threshold We_c separating the "bouncing or coalescence" and "packing I" decreases with increasing droplet diameter. The correlation between We_c and d can be observed from the balance of the energy. For convenience, we assume that the soap film pinches off just as it returns to the initial position. The lower limit of the passing regime means that the velocity of the droplet should be almost zero after pinch-off. This suggests that

$$mgd + mv^2/2 = 2\Delta S\sigma, \tag{1}$$

where $m = \pi\rho d^3/6$ is the mass of the droplet and $\Delta S = \pi d^2$ is the area of the outer shell. Equation (1) can be transformed to $We_c = 24 - 2\kappa^2 d^2$, where $\kappa^{-1} = (\sigma/\rho g)^{1/2}$ is the capillary length of the soap solution. As shown in Fig. 9, it apparently deviates from our results. As we assume that the mass of the soap film is negligible, kinetic energy of the soap film is excluded in Eq. (1). Therefore, the critical Weber number should be higher than the theoretical value. However, this correlation fits well with the reported results.[16,17] This can be attributed to the thinner soap film used in Refs. 16 and 17. The results of the present study fit well with the theoretical line for the large droplets ($d = 3.27$ mm). In this case, mass and kinetic energy of the soap film is insignificant compared with the droplet. The effect of the film thickness is worthy of further investigation.

In the experiments, all of the droplets passing through the soap film are initially enclosed within a shell. However, in the collapsing regime of Fig. 9, the shell collapses immediately after pinch-off. Moreover, the images show that the collapse is related to the vibrations of both the droplet and the soap film, indicating that the time for the droplet to pass through the film is an important factor. We define the contact time t_c as the time from the moment when the soap film first deforms to pinch-off. t_c can be estimated as

$$t_c = (H + d/2)/v, \tag{2}$$

where H is the distance between the mass center of the droplet and the initial soap film. Figure 10 shows the evolution of H with d, where at least eight different impact velocities are included for every drop diameter. The deviation of H increases with the droplet diameter, which can be attributed to the larger oscillating amplitude of the large droplets. The results indicate that $H \sim d$. Le Goff[28] observed a similar relation when a plastic ball collides with soap films which is shown in Fig. 10 as a dashed line. Note that, the length L in Ref. 28 is here equivalent to $H + d/2$ and the dashed line actually indicates $H = 2.5d$ which fits well with our results.

By introducing the scaling time $t_s = (\pi^2\rho d^3/64\sigma)^{1/2}$, the dimensionless contact time $t^* = t_c/t_s$ can be expressed as

$$t^* \sim \frac{d}{v}\sqrt{64\sigma/\pi^2\rho d^3} \sim We^{-1/2}. \tag{3}$$

Here, the scaling time t_s is equivalent to half of the capillary vibration period of the drop. As shown in Fig. 11, Eq. (3) fits the experimental results of all of the drop sizes well. In

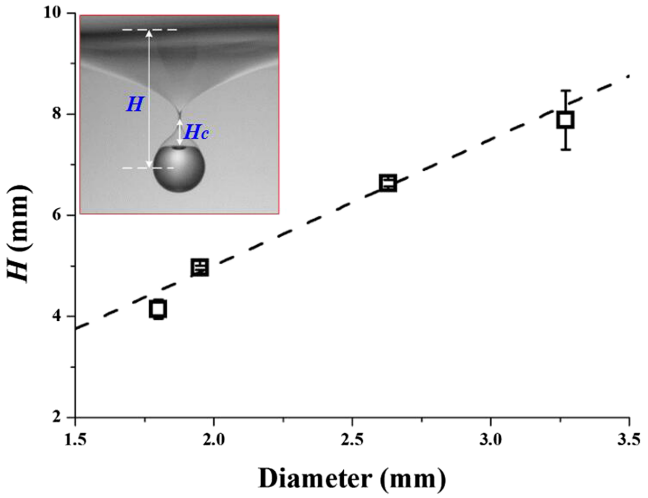

FIG. 10. Evolution of the distance H as a function of the droplet diameter. The dashed line indicates the relation given by Le Goff.[28] The inset shows the definitions of H and H_c.

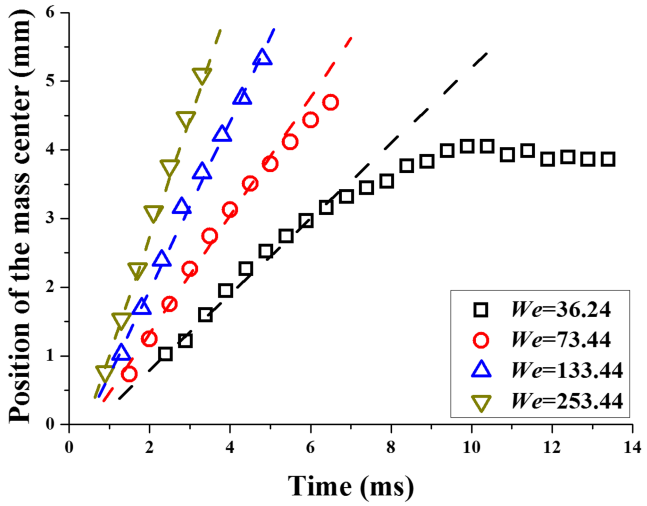

FIG. 12. Evolution of the mass centers of droplets with different impact velocities. All of the diameters are 1.8 mm. The dashed line indicates $s = vt$.

the low Weber number region, the line of $t^* \sim We^{-1/2}$ deviates from the experimental results. This deviation can be attributed to deceleration of the droplet during impact. Figure 12 shows the evolution of the mass centers of droplets with a fixed size ($d = 1.8$ mm) for different impact velocities. The position of the mass center is defined as the distance s between the mass center of the droplet and the initial soap film. The high-speed droplet almost moves with a constant velocity during the collision process, as observed in a previous study.[28] However, the low-speed droplet ($We = 36.24$) significantly decelerates, leading to a longer contact time and the deviation observed in Fig. 11. Note that the experimental results with large droplets ($d = 3.27$ mm) seem to fit well with Eq. (3) even at a lower Weber number. This may be caused by the large deviation of H for the large droplet (Fig. 10).

The contact time plays an important role in the collapse of the outer film. The cases without outer shells after the impact are indicated in red in Fig. 11, showing that the outer shell begins to collapse as t^* decreases to 1. Around this critical t^*, the jet emerging at the top of the droplet begins to puncture the outer shell, as shown in Fig. 5 (Multimedia view). The moment when the jet emerges on the droplet t_J is also a function of We. Figure 13 compares the evolution of t_c and t_J. Note that all of the droplets are of the same size ($d = 1.8$ mm) and their velocities are sufficiently large to pass through the soap film. Apparently, $t_c \le t_J$ is a crucial condition for collapse of the outer shell.

In general, t_c and t_J represent deformation of the soap film and droplet, respectively. When We is very low, t_c is significantly larger than t_J, and the droplet is "packed" after passing through the soap film. With increasing Weber number, t_c and t_J both decrease. However, the contact time t_c decreases faster than t_J, especially in the low-We region. The scaling law is $t_c \sim We^{-1/2}$ [Eq. (3)]. The relation between t_J and We is similar to a droplet falling on a super-hydrophobic surface.[31] In the case of the super-hydrophobic surface, the contact time t_c' is dependent on the impact velocity when the velocity is

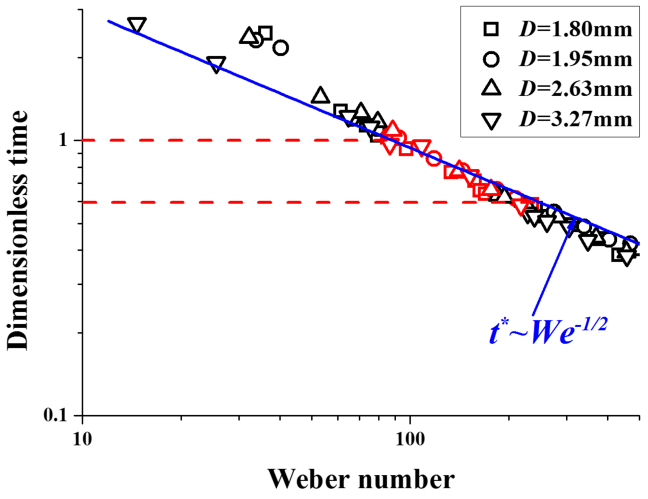

FIG. 11. Relationship between the dimensionless contact time and the Weber number. The black symbols indicate both packing regimes, while the red symbols indicate the collapsing regime. Collapse begins when the dimensionless contact time decreases to 1.

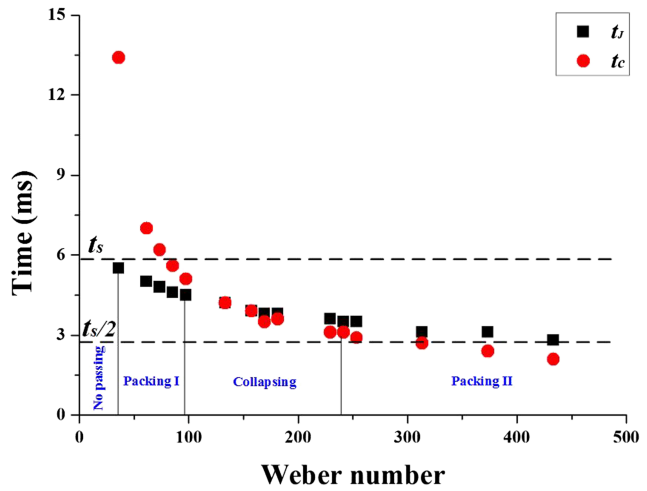

FIG. 13. Evolution of t_c and t_J with the Weber number. Collapse begins when t_c approaches t_J.

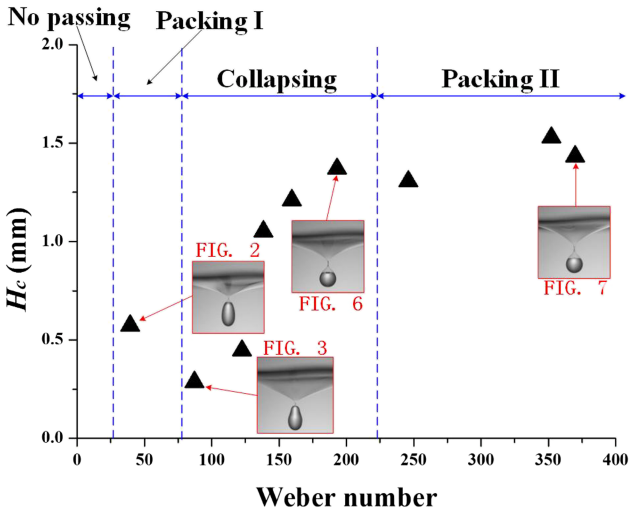

FIG. 14. Relationship between H_c and the Weber number. H_c reaches the minimum value when the packed droplet begins to collapse.

relatively low. With a sufficiently large impact velocity, capillary deformation dominates and t_c' becomes constant.[31] In the low-velocity region, deformation owing to gravity cannot be ignored, causing t_c' to decrease with increasing impact velocity. As shown in Fig. 12, similar evolution of t_J is observed when a droplet collides with a soap film. With increasing *We*, t_J tends to $0.5t_s$. Once *We* becomes greater than a critical value of about 100, the contact time is no longer larger than the jetting time, coinciding with the lower limit of the collapsing regime.

In the region $We > 220$ (packing II regime), the droplet is again packed. This phenomenon can be attributed to two reasons: Firstly, at the moment of separation, the height of the air pocket (H_c, as shown in Fig. 9) increases with increasing impact velocity (Fig. 14). Because collapse of the outer film is caused by the jet at the top of the droplet, it is reasonable that H_c affects the collapse. A larger H_c protects the outer shell, making it harder for the jet to penetrate into the shell. Secondly, during collision between the droplet and the soap film, the transmitted momentum can be expressed as

$$M = \int_0^t F(T)\,dT \sim \sigma dt, \tag{4}$$

where $F(T)$ is the vertical force of the soap film on the droplet.[16] M decreases with decreasing contact time, corresponding to the evolution of the velocity in Fig. 12. As a result, the smaller deformation of the high-speed droplet prevents the outer shell from collapsing.

V. CONCLUSIONS

We have reported experimental results of droplets colliding with a soap film. The critical Weber number for a droplet to pass through the soap film is dependent on its diameter. The contact time decreases with increasing impact velocity. The relation between the contact time and the jetting time plays an important role in the collapse of the packed droplet. In particular, the outer shell begins to collapse when the dimensionless contact time decreases to 1. However, a packed droplet is generated again when the dimensionless contact time decreases to about 0.6.

ACKNOWLEDGMENTS

This work was supported by the National Natural Science Foundation (Grant Nos. 51475415, 51405429, and 51521064), the Zhejiang Provincial Natural Science Foundation for Distinguished Young Scholars (Grant No. LR15E050001), and a Research Project of the State Key Laboratory of Mechanical System and Vibration (Grant No. MSV201706).

[1] J. de Ruiter, R. Lagraauw, D. van den Ende *et al.*, "Wettability-independent bouncing on flat surfaces mediated by thin air films," Nat. Phys. **11**(1), 48–53 (2015).
[2] D. Richard, C. Clanet, and D. Quéré, "Surface phenomena: Contact time of a bouncing drop," Nature **417**(6891), 811 (2002).
[3] C. Antonini, A. Amirfazli, and M. Marengo, "Drop impact and wettability: From hydrophilic to super-hydrophobic surfaces," Phys. Fluids **24**(10), 102104 (2012).
[4] H. N. Oguz and A. Prosperetti, "Bubble entrainment by the impact of drops on liquid surfaces," J. Fluid Mech. **219**, 143–179 (1990).
[5] J. Zou, P. F. Wang, T. R. Zhang *et al.*, "Experimental study of a drop bouncing on a liquid surface," Phys. Fluids **23**(4), 044101 (2011).
[6] H. Lhuissier, C. Sun, A. Prosperetti *et al.*, "Drop fragmentation at impact onto a bath of an immiscible liquid," Phys. Rev. Lett. **110**(26), 264503 (2013).
[7] B. Ching, M. W. Golay, and T. J. Johnson, "Droplet impacts upon liquid surfaces," Science **226**, 535–538 (1984).
[8] W. J. Doak, D. M. Laiacona, G. K. German *et al.*, "Rebound of continuous droplet streams from an immiscible liquid pool. Phys. Fluids **28**(5), 057104 (2016).
[9] J. O. Marston, S. T. Thoroddsen, W. K. Ng *et al.*, "Experimental study of liquid drop impact onto a powder surface," Powder Technol. **203**(2), 223–236 (2010).
[10] Y. S. Joung and C. R. Buie, "Aerosol generation by raindrop impact on soil," Nat. Commun. **6**, 6083 (2015).
[11] M. Rein, "Phenomena of liquid drop impact on solid and liquid surfaces," Fluid Dyn. Res. **12**(2), 61 (1993).
[12] A. L. Yarin, "Drop impact dynamics: Splashing, spreading, receding, bouncing. . . ," Annu. Rev. Fluid Mech. **38**, 159–192 (2006).
[13] C. Josserand and S. T. Thoroddsen, "Drop impact on a solid surface," Annu. Rev. Fluid Mech. **48**, 365–391 (2016).
[14] D. Richard and D. Quéré, "Bouncing water drops," Europhys. Lett. **50**(6), 769 (2000).
[15] C. Clanet, C. Béguin, D. Richard *et al.*, "Maximal deformation of an impacting drop," J. Fluid Mech. **517**, 199–208 (2004).
[16] T. Gilet and J. W. M. Bush, "The fluid trampoline: Droplets bouncing on a soap film," J. Fluid Mech. **625**, 167–203 (2009).
[17] D. Fell, M. Sokuler, A. Lembach *et al.*, "Drop impact on surfactant films and solutions," Colloid Polym. Sci. **291**(8), 1963–1976 (2013).
[18] S. T. Thoroddsen, K. Takehara, T. G. Etoh *et al.*, "Puncturing a drop using surfactants," J. Fluid Mech. **530**, 295–304 (2005).
[19] L. Bai, W. Xu, P. Wu *et al.*, "Formation of antibubbles and multilayer antibubbles," Colloids Surf., A **509**, 334–340 (2016).
[20] S. Dorbolo, H. Caps, and N. Vandewalle, "Fluid instabilities in the birth and death of antibubbles," New J. Phys. **5**(1), 161 (2003).
[21] S. Dorbolo, E. Reyssat, N. Vandewalle *et al.*, "Aging of an antibubble," Europhys. Lett. **69**(6), 966 (2005).
[22] P. G. Kim and H. A. Stone, "Dynamics of the formation of antibubbles," Europhys. Lett. **83**(5), 54001 (2008).
[23] J. Zou, C. Ji, B. G. Yuan *et al.*, "Collapse of an antibubble," Phys. Rev. E **87**(6), 061002 (2013).
[24] D. N. Sob'yanin, "Theory of the antibubble collapse," Phys. Rev. Lett. **114**(10), 104501 (2015).
[25] L. Hu, M. Li, W. Chen *et al.*, "Bubbling behaviors induced by gas-liquid mixture permeating through a porous medium," Phys. Fluids **28**(8), 087102 (2016).

[26]Q. Liu, W. Chen, L. Hu *et al.*, "Experimental investigation of cavity stability for a gas-jet penetrating into a liquid sheet," Phys. Fluids **27**(8), 082106 (2015).
[27]S. Dölle and R. Stannarius, "Microdroplets impinging on freely suspended smectic films: Three impact regimes," Langmuir **31**(23), 6479–6486 (2015).
[28]A. Le Goff, L. Courbin, H. A. Stone *et al.*, "Energy absorption in a bamboo foam," Europhys. Lett. **84**(3), 36001 (2008).
[29]L. Courbin and H. A. Stone, "Impact, puncturing, and the self-healing of soap films," Phys. Fluids **18**(9), 91105 (2006).
[30]P. G. De Gennes, F. Brochard-Wyart, and D. Quéré, *Capillarity and Wetting Phenomena: Drops, Bubbles, Pearls, Waves* (Springer Science & Business Media, 2013).
[31]K. Okumura, F. Chevy, D. Richard *et al.*, "Water spring: A model for bouncing drops," Europhys. Lett. **62**(2), 237 (2003).